PHYSICAL REVIEW A **87**, 031802(R) (2013)

Phonon-mediated electromagnetically induced absorption in hybrid opto-electromechanical systems

Kenan Qu and G. S. Agarwal
Department of Physics, Oklahoma State University, Stillwater, Oklahoma 74078, USA
(Received 21 November 2012; published 18 March 2013)

We predict the existence of the electromagnetically induced absorption (EIA) in the double-cavity configurations of the hybrid opto-electromechanical systems (OEMS). We discuss the origin of the EIA in OEMS which exhibit the existence of an absorption peak within the transparency window. We provide analytical results for the width and the height of the EIA peak. The combination of the electromagnetically induced transparency and EIA is especially useful for photoswitching applications. The EIA that we discuss is different from the one originally discovered by Lezama *et al*. [Phys. Rev. A **59**, 4732 (1999)] in atomic systems and can be understood in terms of the dynamics of three coupled oscillators (rather than two) under different conditions on the relaxation parameters. The EIA we report can also be realized in metamaterials and plasmonic structures.

DOI: 10.1103/PhysRevA.87.031802 PACS number(s): 42.50.Wk, 42.50.Gy

The optomechanical systems have been recognized as good systems for the purpose of optical memories as the mechanical systems can have very long coherence times [1–3]. The realization that such systems can serve as memory elements became feasible by the prediction [4] of electromagnetically induced transparency (EIT) and the experimental demonstration of EIT by several groups [5]. Much of this work was motivated by the corresponding work in atomic media [6]. Although the EIT has been studied extensively in opto-electromechanical systems (OEMS); a counterpart of EIT, namely, the electromagnetically induced absorption (EIA) has not yet been investigated in OEMS. It may be noted that EIT is the result of destructive interference between different pathways leading to suppression of absorption. Thus, one would think that there should be the possibility of constructive interference between different pathways. Such a possibility was first realized by Lezama and co-workers [7] in the context of atomic vapors. More recently, EIT and EIA were demonstrated in plasmonic structures [8] where the interactions and phases can be tailored by design of the structure, thus, enabling one to see either the EIT or the EIA behavior. As we discuss in this Rapid Communication, certain situations do warrant absorption or dispersion as was recognized by Harris and Yamamoto [9] and by Schmidt and Imamoğlu [10]. In this Rapid Communication, we show the existence of EIA in a double-cavity OEMS, thereby, filling a gap that has existed in the physics of OEMS. Such double-cavity configurations are beginning to be studied in a number of papers for different applications [11]. We show how we can switch quite conveniently from EIT to EIA and vice versa by changing the power of the electromagnetic fields. The EIA that we discuss is different as we do not convert the transparency window into an absorption peak, but we create an absorption peak in the transparency window. We note that several recent papers discuss a variety of new effects in double-cavity OEMS. For example, state transfer as well as squeezing using double-cavity OEMS have been studied [11]. Further cavities with many mechanical systems are enabling one to reach very near quantum limit [12].

Lezama and co-workers [7] found that a simple three-level Λ scheme cannot give rise to EIA. They considered optical transitions between the hyperfine states of atoms $F \to F' > F$, which showed the possibility of EIA. The work of Harris and Yamamoto [9] was based on a four-level atomic scheme where one of the ground levels of the Λ scheme was connected by an optical transition to a higher level. This allowed the possibility of two-photon absorption while, at the same time, suppressing one-photon transition. Clearly, if EIA was possible in OEMS, then, we need to consider a more-complicated configuration than, say, considered in the context of EIT: One needs to add an additional pump and, at least, one additional transition. Hence, we study a double-cavity configuration which is flexible enough to open up new pathways for the interaction with the probe field. We would show that the system of Fig. 1 can produce EIA. We show how the EIA in our Rapid Communication can be used to switch transition between two photonic routes in a manner similar to the Zeno effect used in several other types of systems [13]. The switching factor is very large [on the order of 3000 in Fig. 5(a)]. We further show how EIA is useful in the transduction [14] of fields from optical to microwave domain. Our EIA is quite versatile as it would occur in metamaterials [15,16], plasmonics [8,17], or in systems with several mechanical elements [12,18].

The double-cavity configuration, as shown in Fig. 1, has become very popular recently [11] and is becoming key for bringing out very new features of the OEMS. The Hamiltonian for this system is given by

$$\begin{aligned} H &= H_1 + H_2 + H_m + H_{\rm diss}, \\ H_1 &= \hbar(\omega_1 - \omega_{c1})a_1^\dagger a_1 - \hbar g_1 a_1^\dagger a_1 Q + i\hbar\mathcal{E}_{c1}(a_1^\dagger - a_1) \\ &\quad + i\hbar(\mathcal{E}_p a_1^\dagger e^{-i\,\delta t} - \mathcal{E}_p^* a_1 e^{i\,\delta t}), \\ H_2 &= \hbar(\omega_2 - \omega_{c2})a_2^\dagger a_2 + \hbar g_2 a_2^\dagger a_2 Q + i\hbar\mathcal{E}_{c2}(a_2^\dagger - a_2), \\ H_m &= \frac{1}{2}\hbar\omega_m(P^2 + Q^2), \end{aligned} \tag{1}$$

and $H_{\rm diss}$ is corresponding to the dissipation to the Brownian motion of the mechanical resonator with position Q and momentum P normalized such that $[Q, P] = i$ and the leakage of the photons from the cavity. Here, ω_i is the resonant frequency of cavity i, and $\delta = \omega_p - \omega_{c1}$ is the detuning between the probe laser and the coupling laser in cavity 1. Cavity 2 is taken to be a microwave cavity. The coupling rate g_i is defined by $g_i = (\omega_i/L_i)x_{\rm zpf}$ with L_i being the length of the cavity and $x_{\rm zpf} = \sqrt{\hbar/(2m\omega_m)}$ being the zero-point fluctuation for the mechanical resonator. The coupling fields and the probe field inside the cavities are given by $\mathcal{E}_{ci} = \sqrt{2\kappa_i P_i/\hbar\omega_{ci}}$

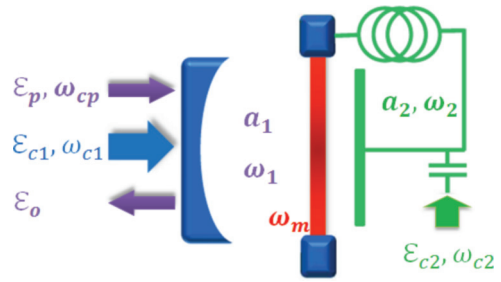

FIG. 1. (Color online) Schematic of the double-cavity OEMS [11].

and $\mathcal{E}_p = \sqrt{2\kappa_1 P_p/\hbar\omega_1}$, respectively. We employ a procedure which is now fairly standard in cavity optomechanics. We obtain the quantum Langevin equations and write the equations for the mean values. The mean-value equations are solved around the steady state by writing all expectation values in the form $A = \sum_{n=-\infty}^{+\infty} e^{-in\,\delta t} A_n$. We obtain A_n's perturbatively. The cavity field a_{i0} is the field in the ith cavity at the frequency of the coupling laser with frequency ω_{ci}. The field $a_{i\pm}$ is the field at the frequency $\omega_{ci} \pm \delta = \omega_{ci} \pm (\omega_p - \omega_{ci})$, and more specifically, $\omega_{1+} = \omega_p$. The output fields resulting from the applied probe field are defined as

$$\mathcal{E}_{o1} = 2\kappa_1(a_{1+}e^{-i(\omega_{c1}+\delta)t} + a_{1-}e^{-i(\omega_{c1}-\delta)t}) - \mathcal{E}_p e^{-i\omega_p t},$$
$$\mathcal{E}_{o2} = 2\kappa_2(a_{2+}e^{-i(\omega_{c2}+\delta)t} + a_{2-}e^{-i(\omega_{c2}-\delta)t}). \quad (2)$$

Note that the component a_{2+} would yield the output at the frequency $\omega_{c2} + \omega_p - \omega_{c1}$, whereas, the component a_{2-} produces an output at the frequency $\omega_{c2} - \omega_p + \omega_{c1}$. We would typically consider the situation when ω_p is close to the cavity frequency and the coupling field ω_{c1} is red detuned by an amount ω_m. The fields ω_{c1} and ω_p combine to produce phonons at the frequency $\omega_p - \omega_{c1} \approx \omega_m$ with $Q_+ \neq 0$. This is the reason for the production of coherent phonons. We now concentrate on the output fields from the two cavities. We display the numerical results for the normalized quantities defined by

$$\mathcal{E}_L = 2\kappa_1 a_{1+}/\mathcal{E}_p, \quad \mathcal{E}_R = 2\kappa_2 a_{2+}/\mathcal{E}_p, \quad (3)$$

which are fields at the frequency of the probe. The actual normalized output field from cavity 1 is given by $(\mathcal{E}_L - 1)$, cf. Eq. (2). We can find that the output is resonantly enhanced when $\delta \sim \Delta_1 = \Delta_2 = \omega_m$, where $\Delta_1 = \omega_1 - \omega_{c1} - g_1 Q_0$ and $\Delta_2 = \omega_2 - \omega_{c2} + g_2 Q_0$. In this regime, both the coupling fields are tuned by an amount ω_m below their corresponding cavity frequency, and the probe laser is in the vicinity of the cavity frequency ω_1. We work in the resolved-side band regime $\omega_m \gg \kappa_{1,2}$. The detailed calculations lead to the following result for the output field $\mathcal{E}_L$:

$$\mathcal{E}_L(x) = \frac{2i\kappa_1}{(x+i\kappa_1) - \frac{g_1^2|a_{10}|^2/2}{(x+i\gamma_m/2) - \frac{g_2^2|a_{20}|^2/2}{(x+i\kappa_2)}}}, \quad (4)$$

where $x(=\delta - \omega_m)$ denotes the detuning of the probe frequency to the cavity frequency. In what follows, we assume that the probe field consists of many photons so that the effect of the thermal photons in the microwave cavity is negligible. In fact, it also turns out that the cooling of the mirror gets enhanced by the coupling field of the second cavity.

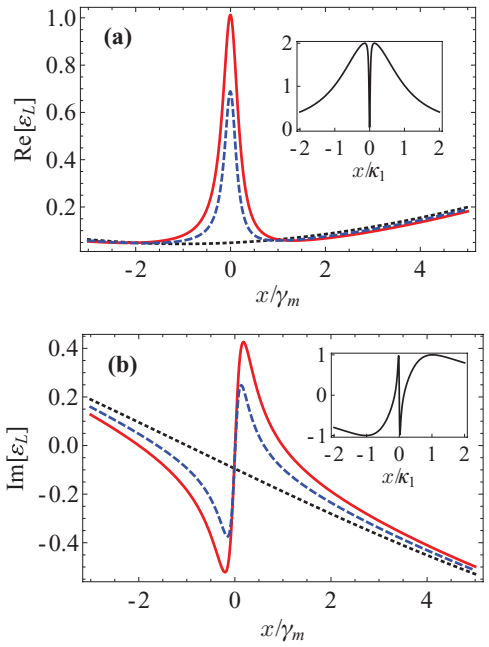

FIG. 2. (Color online) The (a) real and (b) imaginary parts of the field amplitude $\mathcal{E}_L$. The black dotted, blue dashed, and red solid curves are corresponding to the cooperativity ratios $C_2/C_1 = 0, 0.5, 1$, respectively, and $C_1 = 40$. The response shows the effect of EIT when only one coupling field is present, and the emergence of EIA at the line center when both coupling fields are present. The insets show the EIT in a large frequency span with $C_2 = 0$, i.e., with no coupling field applied to the second cavity.

The structure of the output field $\mathcal{E}_L$ is very interesting. It shows how the resonant character of the output field changes from that of an empty cavity ($|a_{10}| = |a_{20}| = 0$) to that of a single cavity ($|a_{20}| = 0$) and to that of double cavities ($|a_{10}| \neq 0$, $|a_{20}| \neq 0$). The denominator in (4) is linear in x (an empty cavity), quadratic in x (a single cavity), and cubic in x (double cavities). These changes determine the physical behavior of the OEMS. In order to explicitly see the nature of the output fields, we use the following set of experimentally realizable parameters: $\omega_{c1} = 2\pi \times 4 \times 10^{14}$ Hz, $\omega_{c2} = 2\pi \times 10$ GHz, $\omega_m = 2\pi \times 10$ MHz, $\gamma_m = 2\pi \times 1$ kHz, $\kappa_1 = 2\pi \times 1$ MHz, $\kappa_2 = 2\pi \times 0.1$ kHz, $g_1 = 2\pi \times 50$ Hz, and $g_2 = 2\pi \times 5$ Hz. In Fig. 2, we show the numerical results for the two quadratures of the output field. These results clearly show the emergence of the EIA within the transparency window. The choice of the parameters to be used is dictated by the structure of (4). We first note that, for $|a_{20}| = 0$, we have the standard EIT behavior (black dotted curves and the insets). We use a coupling power P_{c1} below the critical power defined by $P_{cr} = \frac{\hbar\omega_l}{4g_1^2\kappa_1}(\kappa_1^2 + \omega_m^2)(\frac{\gamma_m}{2} - \kappa_1)^2$ so that, for $P_{c2} = 0$, the two roots for x are purely imaginary. The usual normal-mode splitting [19] occurs when the two roots have nonzero real parts, i.e., $P_{c1} > P_{cr}$. For the parameters above, $P_{cr} \approx 16.6$ mW. For $P_{c1} < P_{cr}$, the interference then leads to the EIT window with a width $\Gamma_{\rm EIT} = (1 + C_1)\gamma_m/2$, where $C_i = g_i^2|a_{i0}|^2/\kappa_i\gamma_m$ denotes the optomechanical cooperativity of cavity i. For the chosen parameters and for $P_{c1} \approx 1.3$ mW, $C_1 = 40$. Clearly, if we want to produce an absorption peak

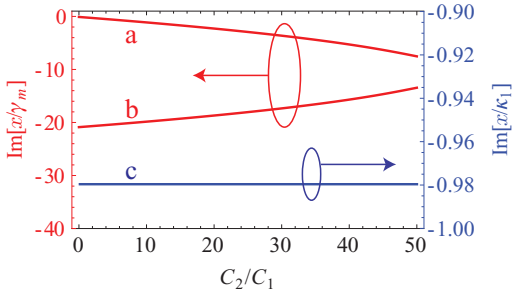

FIG. 3. (Color online) The imaginary part of the roots of Eq. (4) with respect to the ratio C_2/C_1 of the cooperativities of the two cavities and $C_1 = 40$. Their real parts are almost zero.

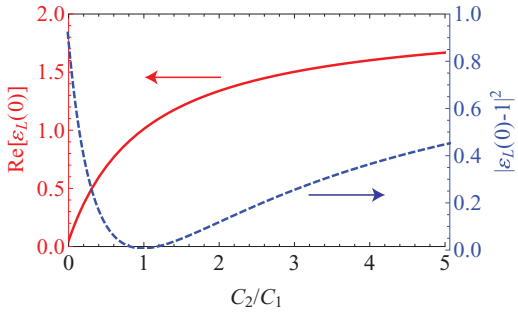

FIG. 4. (Color online) This us the response of the double-cavity OEMS under the effect of coupling fields in both cavities. The solid red curve illustrates the real part of the field amplitude inside the optical cavity at its line center, whereas, its imaginary part is 0. The dashed blue curve illustrates the intensity of the output field from cavity 1 at its line center.

within the EIT window, then we need to choose C_2 such that the third root of the denominator in Eq. (4) lies within the EIT window. For the results shown in Fig. 2, we choose $C_2 = C_1/2$ (blue dashed curves) and $C_2 = C_1$ (red solid curves), corresponding to which $P_{c2} \approx 1.6$ and 3.3 μW. In Fig. 3, we show how the roots of the denominator in Eq. (4) change for P_{c1} below the critical power and if the driving field in cavity 2 is increased. For $C_2 = 0$, the width of the EIT window is $20.5\gamma_m$. Curve **c** gives the overall width within which the transparency window appears. Curve **a** gives the width of the EIA peak within the EIT window. We now examine quantitatively the width of the absorption peak. When $|a_{20}|^2 = 0$, $P_{c1} < P_{cr}$, the two roots of the denominators in (4) are κ_1 and $\Gamma_{\rm EIT}$, and $\Gamma_{\rm EIT} \ll \kappa_1$. In the presence of the additional coupling field $a_{20} \neq 0$, the root $\Gamma_{\rm EIT}$ splits into two parts,

$$\Gamma_{\rm EIT} \to \Gamma_{\pm} = \frac{1}{2}\Gamma_{\rm EIT} \pm \frac{1}{2}\sqrt{\Gamma_{\rm EIT}^2 - 2g_2^2|a_{20}|^2},$$
$$\Gamma_{-} = \Gamma_{\rm EIA} \approx \kappa_2 + \frac{g_2^2|a_{20}|^2}{2\Gamma_{\rm EIT}}, \quad \text{if } \frac{2g_2^2|a_{20}|^2}{\Gamma_{\rm EIT}^2} \ll 1. \tag{5}$$

The existence of an additional splitting in roots $\Gamma_{\pm}$, especially when $\kappa_2 \ll \Gamma_{\rm EIT}$, leads to the absorption peak within the transparency window. The half-width of the absorption peak is given by $\kappa_2 + g_2^2|a_{20}|^2/2\Gamma_{\rm EIT}$. It should be borne in mind that the microwave cavity is especially useful as $\kappa_2 \ll \gamma_m, \Gamma_{\rm EIT}$. Root Γ_- has the behavior given by curve **a** in Fig. 3.

We will now study the characteristics and the origin of the EIA peak. From Eq. (4), we get the height of the EIA peak $\mathcal{E}_L(0) \approx 2/(1 + C_1/C_2)$. Note that the height of the EIA peak depends on the ratio of the cooperativity parameters C_i for the two cavities. We exhibit the behavior of the EIA peak and the output field at the probe frequency $|\mathcal{E}_{o1}(\omega_p)|^2/|\mathcal{E}_p|^2 = |\mathcal{E}_L - 1|^2$ as a function of the ratio of the cooperativity parameters in Fig. 4. Notice from this figure that we get perfect EIA when the ratio of the two cooperativity parameters is unity. At this point, the probe field emerges from the second cavity as displayed in Fig. 5. Figure 5(a) clearly shows how the route of the probe photons changes by the increased absorption resulting from the coupling to the second cavity. This is analogous to the idea of using the Zeno effect [13], i.e., increasing decoherence to switch the path of the photon. According to the procedure outlined after Eq. (1), the probe field produces a steady state of the mechanical mode as $(Q_+e^{-i\omega_m t} + Q_-e^{i\omega_m t})$. Figure 5(b) shows the behavior of the mechanical mode, which goes from a bright mode to an almost dark mode when $C_1 = C_2$. We have concentrated on our demonstration of EIA within the transparency window, although it is possible to have EIA for other ranges of parameters.

Next, we present a coupled oscillator model, which shows the existence of EIA. Note that the coupled oscillator models very often can mimic a variety of physical phenomena. In fact, two coupled oscillators [20] have been used to understand EIT

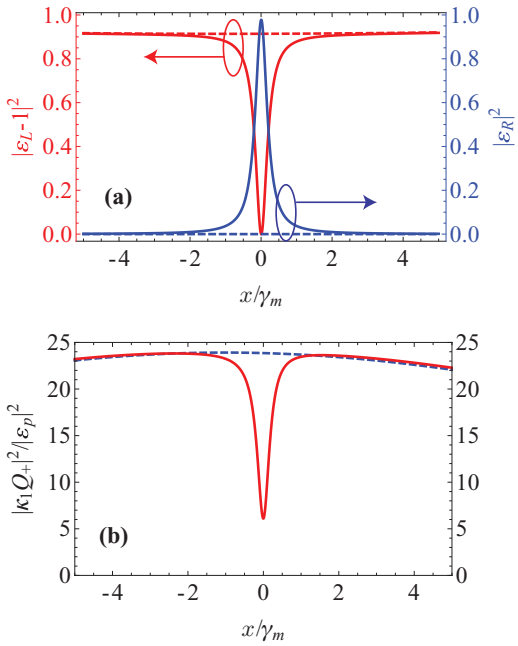

FIG. 5. (Color online) (a) The normalized output from the first cavity $|\mathcal{E}_L - 1|^2$ and from the second cavity $|\mathcal{E}_R|^2$ and (b) the amplitude of the mechanical displacement normalized to $|\mathcal{E}_p|^2$. The system behaves (almost) as a perfect reflection with a bright mechanical mode when dashed curves: $C_2 = 0$; and it behaves as a perfect transmission with a nearly dark mechanical mode when solid curves: $C_2 = C_1$.

as well as EIA [7,8]. It turns out that the EIA of the type discussed in this Rapid Communication has to be understood in terms of three coupled oscillators—in our case, two of these (u and v) would represent cavity modes, and the third one (w) would represent the mechanical oscillator. The three effective oscillators can be described by equations (written in rotating-wave approximation) as

$$\begin{aligned} \dot{u} &= -i\,\Delta_1 u - iG_1 w - \kappa_1 u + \mathcal{E}_p e^{-i\,\delta t}, \\ \dot{v} &= -i\,\Delta_2 v - iG_2 w - \kappa_2 v, \\ \dot{w} &= -i\omega_m w - iG_1 u - iG_2 v - (\gamma_m/2)w. \end{aligned} \tag{6}$$

These three coupled equations can exhibit a variety of phenomena depending on the couplings G_1, G_2 and the relaxation parameters κ_1, κ_2 and γ_m. For the existence of the EIA, it is simple to have $\kappa_1 \gg \gamma_m \gg \kappa_2$. Note that a whole class of hybrid systems coupling optical and microwave systems can be described by Eqs. (6) and their quantum version in terms of Langevin equations [21].

In conclusion, we have demonstrated the possibility of the EIA within the transparency window of the optomechanical systems. For the OEMS of this Rapid Communication, the EIA results in the transduction of optical fields to microwave fields. Note, however, that the transduction of fields at single-photon levels would require a full quantum treatment as in Ref. [2], although the quantum ground state is now realized [22]. The EIA within the transparency window is quite generic and is applicable to a variety of systems, which can effectively be described by three coupled oscillators. These systems would include other types of optomechanical systems, such as those containing two mechanical elements [12,18], two qubits [23], or very different classes of systems, such as plasmonic structures [8,17] and metamaterials [15,16]. Further, the three-oscillator model can be shown to lead to double Fano resonances.

G.S.A. would like to thank Tata Institute of Fundamental Research, Mumbai, where part of this work was performed.

[1] A. I. Lvovsky, B. C. Sanders, and W. Tittel, Nat. Photonics **3**, 706 (2009).
[2] G. S. Agarwal and S. Huang, Phys. Rev. A **85**, 021801(R) (2012).
[3] V. Fiore *et al.*, Phys. Rev. Lett. **107**, 133601 (2011); E. Verhagen, S. Delélise, S. Weis, A. Schliesser, and T. J. Kippenberg, Nature (London) **482**, 63 (2012).
[4] G. S. Agarwal and S. Huang, Phys. Rev. A **81**, 041803(R) (2010).
[5] S. Weis *et al.*, Science **330**, 1520 (2010); Q. Lin *et al.*, Nat. Photonics **4**, 236 (2010); A. H. Safavi-Naeini *et al.*, Nature (London) **472**, 69 (2011); J. D. Teufel *et al.*, *ibid.* **471**, 204 (2011).
[6] S. E. Harris, Phys. Today **50**(7), 36 (1997); S. E. Harris, J. E. Field, and A. Imamoğlu, Phys. Rev. Lett. **64**, 1107 (1990).
[7] A. Lezama, S. Barreiro, and A. M. Akulshin, Phys. Rev. A **59**, 4732 (1999); A. M. Akulshin, S. Barreiro, and A. Lezama, *ibid.* **57**, 2996 (1998); A. Lipsich, S. Barreiro, A. M. Akulshin, and A. Lezama, *ibid.* **61**, 053803 (2000).
[8] R. D. Kekatpure, E. S. Barnard, W. Cai, and M. L. Brongersma, Phys. Rev. Lett. **104**, 243902 (2010); R. Taubert, M. Hentschel, J. Kästel, and H. Giessen, Nano Lett. **12**, 1367 (2012).
[9] S. E. Harris and Y. Yamamoto, Phys. Rev. Lett. **81**, 3611 (1998).
[10] H. Schmidt and A. Imamoğlu, Opt. Lett. **21**, 1936 (1996).
[11] C. A. Regal and K. W. Lehnert, J. Phys.: Conf. Ser. **264**, 012025 (2011); Y. D. Wang and A. A. Clerk, Phys. Rev. Lett. **108**, 153603 (2012); L. Tian, *ibid.* **108**, 153604 (2012); S. Barzanjeh, M. Abdi, G. J. Milburn, P. Tombesi, and D. Vitali, *ibid.* **109**, 130503 (2012).
[12] F. Massel, S. U. Cho, J.-M. Pirkkalainen, P. J. Hakonen, T. T. Heikkilä, and M. A. Sillanpää, Nat. Commun. **3**, 987 (2012).
[13] K. T. McCusker, Y.-P. Huang, A. Kowligy, P. Kumar, arXiv:1301.7631 (2013); Y. H. Wen, O. Kuzucu, M. Fridman, A. L. Gaeta, L.-W. Luo, and M. Lipson, Phys. Rev. Lett. **108**, 223907 (2012); B. C. Jacobs and J. D. Franson, Phys. Rev. A **79**, 063830 (2009).
[14] T. Faust, P. Krenn, S. Manus, J. P. Kotthaus, and E. M. Weig, Nat. Commun. **3**, 728 (2012).
[15] R. Singh, C. Rockstuhl, F. Lederer, and W. Zhang, Phys. Rev. B **79**, 085111 (2009); J. Gu *et al.*, Nat. Commun. **3**, 1151 (2012).
[16] Our current simulations, using a three-layer metamaterial structure at terahertz frequencies, have already established the existence of EIA along the lines predicted by Eq. (6); W. Zhang *et al.* (unpublished).
[17] B. Gallinet and O. J. F. Martin, ACS Nano **5**, 8999 (2011).
[18] S. Huang and G. S. Agarwal, New J. Phys. **11**, 103044 (2009); M. Bhattacharya, H. Uys, and P. Meystre, Phys. Rev. A **77**, 033819 (2008); M. J. Hartmann and M. B. Plenio, Phys. Rev. Lett. **101**, 200503 (2008).
[19] J. M. Dobrindt, I. Wilson-Rae, and T. J. Kippenberg, Phys. Rev. Lett. **101**, 263602 (2008); S. Grölacher, K. Hammerer, M. R. Vanner, and M. Aspelmeyer, Nature (London) **460**, 724 (2009).
[20] C. L. Garrido Alzar, M. A. G. Martinez, and P. Nussenzveig, Am. J. Phys. **70**, 37 (2002); D. D. Smith, H. Chang, K. A. Fuller, A. T. Rosenberger, and R. W. Boyd, Phys. Rev. A **69**, 063804 (2004); A. Naweed, G. Farca, S. I. Shopova, and A. T. Rosenberger, *ibid.* **71**, 043804 (2005); K. Totsuka, N. Kobayashi, and M. Tomita, Phys. Rev. Lett. **98**, 213904 (2007).
[21] X. Zhu *et al.*, Nature (London) **478**, 221 (2011).
[22] J. D. Teufel *et al.*, Nature (London) **475**, 359 (2011).
[23] F. Altomare *et al.*, Nat. Phys. **6**, 777 (2010).